RSCPublishing

COMMUNICATION
Leroy Cronin *et al.*
Configurable 3D-Printed millifluidic and microfluidic 'lab on a chip'
reactionware devices

COMMUNICATION

Configurable 3D-Printed millifluidic and microfluidic 'lab on a chip' reactionware devices†

Philip J. Kitson, Mali H. Rosnes, Victor Sans, Vincenza Dragone and Leroy Cronin*

We utilise 3D design and 3D printing techniques to fabricate a number of miniaturised fluidic 'reactionware' devices for chemical syntheses in just a few hours, using inexpensive materials producing reliable and robust reactors. Both two and three inlet reactors could be assembled, as well as one-inlet devices with reactant 'silos' allowing the introduction of reactants during the fabrication process of the device. To demonstrate the utility and versatility of these devices organic (reductive amination and alkylation reactions), inorganic (large polyoxometalate synthesis) and materials (gold nanoparticle synthesis) processes were efficiently carried out in the printed devices.

Introduction

The realisation of rapidly configurable and scalable reactor devices for the exploration of complex chemical systems is a highly sought after target.[1] In particular the development of precision micro-to-milli-scale fluidic devices that are configurable 'on-the-fly' is an area of much current interest.[2] The high surface area-to-volume ratio, precise control, and manipulation of reaction environment that can be achieved at these dimensions is critical for lab-on-a-chip devices, but 3D printing technologies have hitherto been overlooked in this area due to a perceived limitation of resolution. Depending on the reactor dimensions these devices can be classed as either nano- (1–100 nm), micro- (100 nm to 1 mm) or milli-fluidics (1–10 mm).[3] As such we hypothesised that the assembly of 3D printed larger scale, 'milli' fluidic reactors, could allow the rapid fabrication of a range of versatile devices. For millifluidics, while the surface-area-to-volume ratio remains high, the pressure drop within reactors is much lower than in microfluidics and problems typically associated with microfluidics, such as blockages due to the formation of precipitates, are greatly mitigated.[4] Also, one of the major drawbacks of these miniaturised structures is that the production of such devices tends to be time consuming. Herein we present a facile approach to the fabrication of intricate micro- and milli-fluidic devices, which allows the entire process from initial design to functional reactor to be completed in a matter of hours using low cost materials.

In the last few decades the precision manufacturing of chemical devices has been utilised in analytical chemistry, chemical engineering, and process optimisation. In general such devices have been machined in a variety of materials including steel, silicon and plastic. For instance the injection moulding of plastic has allowed a range of diverse devices to be constructed but these techniques require rather specialised fabrication facilities, and can be costly and time consuming.[4]

Three-dimensional (3D) printing has long been used in manufacturing industries to produce design prototypes, however it is only relatively recently that these technologies have developed to the degree where they can produce functional devices in their own right,[5] such as tissue growth scaffolds,[6] prototyping,[7] electronics,[8] microfluidics[9] and pneumatics.[10] We have previously reported the use of 3D printing to initiate chemical reactions by printing reagents directly into a 3D 'reactionware' matrix (reactionware refers to devices that combine both reactor and reagent, catalytic or architectural control of the reaction outcome).[11] Here we show how 3D printing can be used to make intricate micro- and milli- scale reactionware. This methodology offers significant freedom to design bespoke reactors in terms of residence time, mixing points, inlets and outlets, *etc.* Due to the ease of fabrication this approach also facilitates quick production turn-around, allowing the design of such devices to be iterated and optimised rapidly based on experimental data.

Results

To demonstrate the high versatility of low-cost 3D printing techniques in the fabrication of micro- and milli-fluidic devices, we printed devices which were successfully used to perform organic, inorganic, and materials syntheses. This establishes the extraordinary possibilities offered by the application of 3D printing, and in particular our invention of the reactionware concept and its application at this scale.[11] Our devices were designed using a freely distributed 3D Computer Aided Design (CAD) software package (Autodesk123D) and the devices presented were printed in polypropylene (PP) using a 3DTouch™ printer which deposits layers of thermopolymers through heated extruder nozzles to build up the desired 3D architectures (see Fig. 1).

School of Chemistry, University of Glasgow, G12 8QQ, United Kingdom. E-mail: Lee.Cronin@glasgow.ac.uk www.croninlab.com
† Electronic Supplementary Information (ESI) available. See DOI: 10.1039/c2lc40761b

Fig. 1 (Left) Schematic drawing of the design of one of the reactors used in this study. (Centre) 3DTouch™ 3D printer used in the fabrication of the micro- and milli-reactors. (Right) device printed from the drawing shown on the left. The channels in the device have been filled with a methanol solution of Rhodamine B dye to render them visible, and the dye can be completely removed by subsequent washing.

PP is an attractive material for the fabrication of micro- and milli-scale reactionware as it is a robust, flexible and chemically inert polymer, and is significantly less expensive than materials which are often used in the synthesis of such small devices, such as polydimethylsiloxane (PDMS). The price of PP is about US$ 0.02 per gram; hence the maximum price for the material used in the devices presented in this article is about US$ 0.31.

Three example devices are presented here (see Fig. 2). The first reactor (R1) is a two inlet device with an approximate reactor volume (V_R) of 60 μL. The second device (R2) is a three inlet reactor, which has two initial inlets which are joined by a third inlet after a reaction volume of approximately 270 μL. The third piece of reactionware (R3) represents a reactor which would be difficult to fabricate using traditional methods of production of micro- to milli-scale reactors (for example the soft-lithographic processing of PDMS). R3 incorporates reactant 'silos' which are filled with the desired reactants during the fabrication of the device. A solution can then be introduced into the reactor by a single inlet and induced to flow through the device dissolving first one, and then the other reactant to effect a chemical reaction. Each device proved
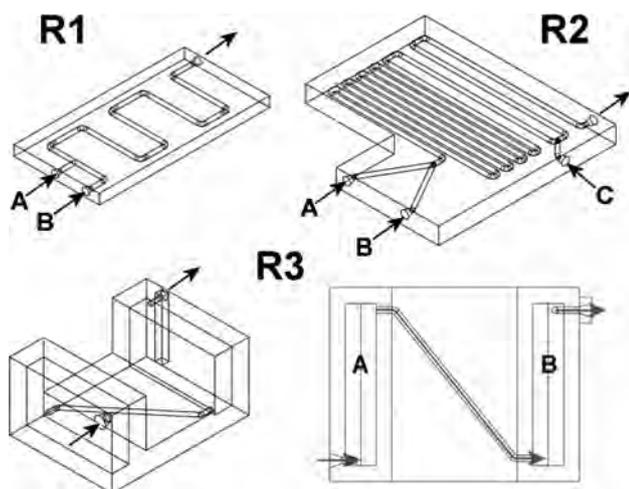
to be robust and versatile, and R1 and R2 could be recycled for use multiple times.

The 3D printer used in this work has a print tolerance of $\pm$ 0.2 mm and the Z resolution (*i.e.* the height of each layer of deposited thermopolymer) of the printer is 0.125 mm ($\pm$ 0.06 mm), allowing the printing of channels which are approximately circular in cross section and with a channel diameter of approximately 0.8 mm, as determined by optical microscopy of half-printed channels (see Fig. 3). The printing of the devices took less than 4 h for even the largest device design (R3), and before any reactions were initiated the reactors (R1 and R2) were tested using a dye solution of Rhodamine B in methanol, to confirm that the devices had been printed accurately and that there were no leaks in the channel systems.

A summary of the time and costs associated with each of the three reactors is given in Table 1. The heaviest reactor was R3, weighing 13.38 g. For R1 and R2 the cost was less, demonstrating
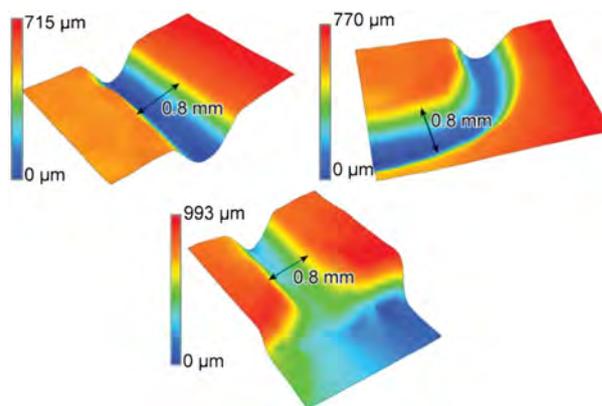

Fig. 3 3D profiles of various features obtained by optical microscopy of half-printed channels; (top left) a typical straight channel, (top right) 90° bend in a channel, (below) opening of a channel at the wall of a device.

the potential for 3D printing technologies to produce millifluidic reactors at very low materials cost. Another benefit of this approach to micro- and milli-reactionware fabrication was the speed of printing; traditionally the fabrication of micro- and milli-reactors is a slow process where it is time consuming to alter the design and fabricate new and improved devices if faults or errors are detected. For the 3D-printed devices presented herein, we could easily alter or re-design the devices, and reprint them within a few hours (see Table 1).

To carry out reactions, 1/16″ outer diameter (OD) PTFE-tubing was attached to the inlet and outlet openings of each device using commercial epoxy adhesive. This tubing was then fitted with

Fig. 2 CAD drawings of each of the three devices; (top left) R1; A two-inlet device, (top right), R2; a three-inlet device, (below) R3; a one-inlet device with two "silos": one filled with sodium molybdate (A) and the other with hydrazine dihydrochloride (B), both as solids. An oblique and aerial view are provided. The arrows indicate the various inlets and outlets.

Table 1 An overview of the time and cost associated with the fabrication of each of the three reactors, along with their overall dimensions

	R1	R2	R3
Printing Time (h)	2	4	4
Reactor Weight (g)	3.9	8.8	13.4
Printing Materials Cost (US$)	0.09	0.20	0.31
Dimensions (mm)	25 × 50 × 3	56 × 52 × 6	40 × 30 × 20

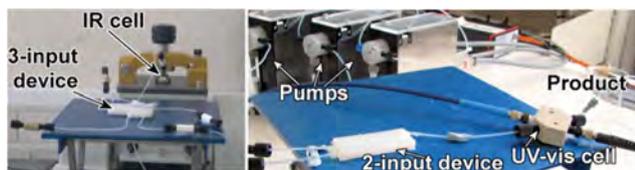This journal is © The Royal Society of Chemistry 2012

Fig. 4 The actual set-up of the devices, with three inlets each connected to a pump, and the in-line ATR-IR and/or UV-Vis flow-cells connected to the outlet.

standard connectors allowing the device inlets to be connected to pumps containing the necessary starting materials, and allowing the device outlets to be connected to in-line analytical instruments appropriate to the experiment being performed, in this case either IR or UV-Vis spectroscopy (see Fig. 4). This could be done as soon as the device had been printed.

As an exemplar reaction, we decided to utilise R1 for sequential imine formation and reduction. To do this, the inlets were
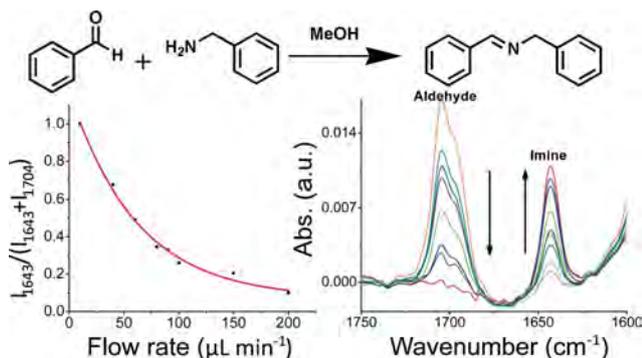

Fig. 5 Flow synthesis of the imine derived from benzaldehyde and benzylamine, as characterised by in-line ATR-IR spectroscopy.

connected to pump-controlled syringes charged with 1 M methanolic solutions of benzylamine (inlet A) and benzaldehyde (inlet B).[12] The outlet of the reactor was then connected to an IR spectrometer and the progress of the reaction was followed by flow ATR-IR spectroscopy. This technique has proven very useful for the characterization of organic reactions under flow conditions.[13,14] By comparing the spectra obtained to that of benzaldehyde, it is evident that the peak due to the presence of the aldehyde moiety disappears as the peak due to the imine moiety appears (see Fig. 5). At a total flow rate of 10 μL min^{-1} full conversion to the imine was observed whereas at higher flow rates the conversion decreased as expected due to the reduced residence time of the reactants within the device. ^{1}H NMR confirmed the presence of the imine as the sole product (see ESI). Hence, the IR absorbances due to the presence of the imine and aldehyde could be employed to monitor the progress of the reaction as a function of the flow rate.

To further demonstrate the scope of our reactors to conduct organic reactions, we employed the three inlet device, R2 (Fig. 6 LHS), to carry out a reductive amination under flow conditions. There are only a few previous examples of such reductions employing microstructured devices.[13,15–17] In this case, the reductive amination was carried out by connecting the initial

inlets of the device to the same solutions of benzylamine (inlet A) and benzaldehyde (inlet B) as previously employed, at a low flow rate (5 μL min^{-1}), allowing the solutions to react in the first section of the reactor. At this flow rate, a residence time of *ca.* 42 min ensured full conversion to the imine. A 1 M solution of sodium cyanoborohydride was then introduced through the third inlet (inlet C) at 2.5 μL min^{-1} to reduce the imine to a secondary amine. Under these conditions, the complete disappearance of aldehyde and imine absorbances by ATR-IR confirmed the full conversion of the substrates (see ESI Fig. S4). Unfortunately, the secondary amine does not produce a significant IR vibration. However MS spectroscopy, and TLC, confirmed the formation of the secondary amine.

In addition, the same reactor device could be employed for an alkylation reaction. Sodium cyanoborohydride does not react with aldehyde functionalities, so it could be introduced into the device together with the benzaldehyde solution, *via* inlet B. Under these conditions, the complete disappearance of aldehyde and imine absorbances by ATR-IR again confirmed the full conversion to the secondary amine. We then introduced a methanolic solution of allyl bromide *via* inlet C to carry out an alkylation of the secondary amine, as confirmed by mass spectrometry (MS) and TLC analysis (see the ESI for further details).

After successfully carrying out a range of organic transformations, it was decided to explore inorganic reactions, to demonstrate the synthetic scope of 3D-printed reactors, especially for complex 'one-pot' self-assembly reactions. This builds upon our recent work demonstrating the possibility of synthesizing polyoxometalates (POMs) in a flow set-up.[18] Hence, we assessed the suitability of the printed reactionware for synthesizing POMs. To this end, we employed reactor R2, introducing 1 M HCl$_{(aq)}$ *via* inlet A, sodium molybdate (0.625 M) *via* inlet B and the reducing agent hydrazine dihydrochloride (0.12 M) *via* inlet C. An in-line UV-Vis spectrometer was used to monitor the transformation. At first only inlet A and B were active, hence only HCl and sodium molybdate were employed, and as expected $[Mo_{36}O_{112}(H_2O)_{16}]^{8-}$, {Mo$_{36}$}, was produced as evidenced by time dependent flow UV-Vis and DLS;[19] this also showed that the product was stable over time, as demonstrated by the stable absorbance band at 340 nm (see ESI Fig. S6). We then activated inlet C, and introduced the reducing agent, and the spectra quickly changed to show a new band at 750 nm, confirming that the {Mo$_{36}$} had been partially reduced, forming molybdenum blue $[Mo_{154}O_{462}H_{14}(H_2O)_{70}]^{14-}$, {Mo$_{154}$}[19]

Fig. 6 Physical set-up of the 3D-printed reactionware used in the polyoxometalate syntheses. (Left) Three inlet device (R2) used with inlets of Na$_2$MoO$_4$·2H$_2$O, HCl$_{(aq)}$ and NH$_2$NH$_2$·2HCl. (Right) One inlet device (R3) where HCl is flowed through silos containing solid Na$_2$MoO$_4$·2H$_2$O and hydrazine dihydrochloride, respectively.
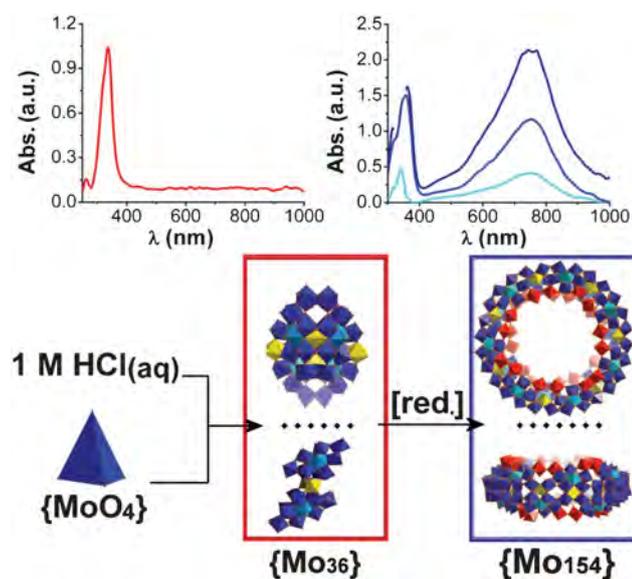
Fig. 7 (Top Left) UV-Vis spectrum corresponding to the {Mo₃₆} cluster, and (top right) UV-Vis spectrum corresponding to the giant cluster {Mo₁₅₄} under flow conditions employing a 3D-printed reactor (R2). flow rates: Light blue 75 μL min⁻¹, blue 37.5 μL min⁻¹, navy 18.25 μL min⁻¹ (Bottom) The reaction pattern of sodium molybdate, in the presence of acid, to {Mo₃₆}, and then in the presence of a reducing agent to form {Mo₁₅₄} (see ESI Fig. S7).

(see ESI Fig. S7). DLS and UV-Vis spectroscopy of the samples collected confirmed the presence of {Mo₃₆} in the absence of reducing agent and {Mo₁₅₄} in the presence of reducing agent, respectively (see Fig. 7). For the {Mo₃₆}, sample particles of a hydrodynamic diameter of 1.5 nm were observed, whilst a diameter of 3.6 nm was found in the case of {Mo₁₅₄} (see ESI Fig. S8). These values are slightly lower than the reported values of 1.9 and 3.9 nm respectively.[19]

To expand on the concept of inorganic reactions, along with in-built materials in pre-designed matrices, we designed a new type of device (R3, see Fig. 6 RHS), where small containers for solid material were included and filled with reagents before the devices were completed on the 3D-printer, *i.e.* a device with inbuilt reagents. During the 3D printing process, the printing was paused and solid sodium molybdate (Na₂MoO₄·2H₂O, 300 mg, 1.24 mmol) and hydrazine dihydrochloride (NH₂NH₂·2HCl, 20 mg, 0.19 mmol) were deposited in the first (A in Fig. 2) and second (B) reactant chambers respectively. Printing of the device was then resumed and, once completed, the device was connected with
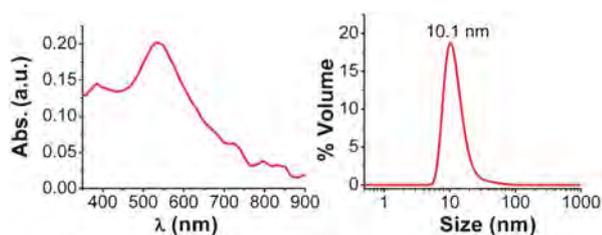

Fig. 8 Synthesis of Au nanoparticles employing 3D-printed reactor R1. (Left) Absorption spectrum acquired by in-line UV-Vis λ_{max}=537nm. (Right) Particle size determination was achieved by DLS.

PTFE tubing as described above. Aqueous hydrochloric acid (pH 1) was then introduced into the reactor *via* the only inlet into the first chamber (A), dissolving the solid sodium molybdate before moving on to the second chamber (B), where the reducing agent was present as a solid. The reaction mixture then flowed through the outlet, and UV-Vis spectroscopy and DLS analysis were used to confirm the presence of the {Mo₁₅₄} in the product stream.

Finally, the 3D-printed reactors could be used to synthesise gold nanoparticles. To achieve this, R1 was employed as the reactor, with a (1 : 1) mixture of aqueous solutions of HAuCl₄ (0.2 mM) and sodium citrate (2 mM) introduced through the first inlet of the device. Simultaneously an aqueous solution of NaBH₄ (10 mM) was introduced through the second inlet. The reaction was monitored by in-line UV-Vis spectroscopy where the formation of gold nanoparticles could be clearly observed by monitoring a peak in the absorption spectrum with a maximum at 537 nm. DLS confirmed the presence of nanoparticles with a particle size of 10 nm (see Fig. 8). The intensity of the observed UV-Vis spectrum decreased over time, probably due to the deposition of gold on the reactor walls. This effect has been previously reported by Koehler *et al.*[20] and could be used in the future as a way to modify the interior surfaces of such devices to impart further functionality on these architectures.

Conclusions

In conclusion, we have demonstrated the viability, versatility, and configurability of 3D printing in the fabrication of miniaturised reactors. Within the timespan of one day, a geometry tailored to a specific reaction was designed, printed in a suitable material, and used to perform organic, inorganic or materials syntheses. The material used for the fabrication of these devices was inexpensive and provided a suitably inert material for the reactions performed. As an added benefit, due to the time and cost-effectiveness of this type of fabrication technique for the production of millifluidic devices, it proved straightforward to alter the design of the devices in terms of geometry, inlets, outlets and sizes of channels. This is very rare with traditional fluidic devices, where redesign and refabrication of devices can be time consuming. Several chemical syntheses have been efficiently carried out in the devices described in this paper; organic synthesis of an amine by two-step reductive amination, and subsequent alkylation of the resulting secondary amine; the inorganic synthesis of large polyoxometalate clusters; and the controlled synthesis of gold nanoparticles. Along with these, we have demonstrated the scope for the realization of novel reactor architectures inherent in the 3D printing of such reactors by the design, fabrication and use of a type of reactionware (R3) in which the reactants were incorporated during the fabrication process itself, a feat which would be extremely difficult using traditional methods of production.

We think that the scope for 3D-printed milli-devices is huge, and to highlight this potential further, we are currently working towards expanding the versatility of the devices. In particular we are aiming to explore the incorporation of transparent observation windows, solvent compatibility, increasing connectivity, *in situ* and extended in-line analysis, temperature control, increased temperature range, active materials, *etc.*, and we will further develop this in later work, especially in relation to complex chemical systems and integrated bio-and-chemo-reactionware.

Acknowledgements

References

1 G. J. T. Cooper, P. J. Kitson, R. S. Winter, M. Zagnoni, D.-L. Long and L. Cronin, *Angew. Chem., Int. Ed.*, 2011, **50**, 10373.
2 A. Waldbaur, H. Rapp, K. Lange and B. E. Rapp, *Anal. Methods*, 2011, **3**, 2681–2716.
3 (*a*) T. Illg, P. Lob and V. Hessel, *Bioorg. Med. Chem.*, 2010, **18**, 3707–3719; (*b*) Y. Li, A. Sanampudi, V. Raji Reddy, S. Biswas, K. Nandakumar, D. Yemane, J. Goettert and C. S. S. R. Kumar, *ChemPhysChem*, 2012, **13**, 177–182.
4 J. P. Hulme, S. Mohr, N. J. Goddard and P. R. Fielden, *Lab Chip*, 2002, **2**, 203.
5 P. Marks, M. Campbell, J. Aron and H. Lipson, *New Sci.*, 2011, **2823**, 17–20.
6 J. N. Hanson Shepherd, S. T. Parker, R. F. Shepherd, M. U. Gillette, J. A. Lewis and R. G. Nuzzo, *Adv. Funct. Mater.*, 2011, **21**, 47–54.
7 J. Stampfl and R. Liska, *Macromol. Chem. Phys.*, 2005, **206**, 1253–1256.
8 B. Y. Ahn, E. B. Duoss, M. J. Motala, X. Guo, S.-I. Park, Y. Xiong, J. Yoon, R. G. Nuzzo, J. A. Rogers and J. A. Lewis, *Science*, 2009, **323**, 1590–1593.
9 D. Therriault, S. R. White and J. A. Lewis, *Nat. Mater.*, 2003, **2**, 265–271.
10 F. Ilievski, A. D. Mazzeo, R. F. Shepherd, X. Chen and G. M. Whitesides, *Angew. Chem., Int. Ed.*, 2011, **50**, 1890–1895.
11 M. D. Symes, P. J. Kitson, J. Yan, C. J. Richmond, G. J. T. Cooper, R. W. Bowman, T. Vilbrandt and L. Cronin, *Nat. Chem.*, 2012, **4**, 349–354.
12 H. Wensink, F. Benito-Lopez, D. C. Hermes, W. Verboom, H. J. G. E. Gardeniers, D. N. Reinhoudt and A. van den Berg, *Lab Chip*, 2005, **5**, 280–284.
13 C. F. Carter, H. Lange, S. V. Ley, I. R. Baxendale, B. Wittkamp, J. G. Goode and N. L. Gaunt, *Org. Process Res. Dev.*, 2010, **14**, 393–404.
14 Z. Qian, I. R. Baxendale and S. V. Ley, *Chem. Eur. J.*, 2010, **16**, 12342–12348.
15 S. Saaby, K. R. Knudsen, M. Ladlow and S. V. Ley, *Chem. Commun.*, 2005, 2909–2911.
16 J. Sedelmeier, S. V. Ley and I. R. Baxendale, *Green Chem.*, 2009, **11**, 683–685.
17 X. Fan, V. Sans, P. Yaseneva, D. D. Plaza, J. Williams and A. Lapkin, *Org. Process Res. Dev.*, 2012, **16**, 1039–1042.
18 H. N. Miras, G. J. T. Cooper, D. L. Long, H. Bögge, A. Müller, C. Streb and L. Cronin, *Science*, 2010, **327**, 72–74.
19 H. N. Miras, C. J. Richmond, D. L. Long and L. Cronin, *J. Am. Chem. Soc.*, 2012, **134**, 3816–3824.
20 J. Wagner and J. M. Köhler, *Nano Lett.*, 2005, **5**, 685–691.